

Nanoscale

Accepted Manuscript



This is an *Accepted Manuscript*, which has been through the Royal Society of Chemistry peer review process and has been accepted for publication.

Accepted Manuscripts are published online shortly after acceptance, before technical editing, formatting and proof reading. Using this free service, authors can make their results available to the community, in citable form, before we publish the edited article. We will replace this *Accepted Manuscript* with the edited and formatted *Advance Article* as soon as it is available.

You can find more information about *Accepted Manuscripts* in the [Information for Authors](#).

Please note that technical editing may introduce minor changes to the text and/or graphics, which may alter content. The journal's standard [Terms & Conditions](#) and the [Ethical guidelines](#) still apply. In no event shall the Royal Society of Chemistry be held responsible for any errors or omissions in this *Accepted Manuscript* or any consequences arising from the use of any information it contains.

Cite this: DOI: 10.1039/c0xx00000x

www.rsc.org/xxxxxx

ARTICLE TYPE

One-pot Hydrothermal Synthesis of Peony-like Ag/Ag_{0.68}V₂O₅ Hybrid as High-Performance Anode and Cathode Materials for Rechargeable Lithium Batteries

Denghu Wei,^{†a} Xiaona Li,^{†a} Yongchun Zhu,^{*a} Jianwen Liang,^a Kailong Zhang,^a and Yitai Qian ^{*a,b}⁵ Received (in XXX, XXX) Xth XXXXXXXXXX 20XX, Accepted Xth XXXXXXXXXX 20XX

DOI: 10.1039/b000000x

Peony-like Ag/Ag_{0.68}V₂O₅ hybrid assembled from nanosheets with the thickness of 40 nm was synthesized through a one-pot hydrothermal approach from vanadium pentoxide (V₂O₅), oxalic acid (H₂C₂O₄), and silver nitrate (AgNO₃) at 180 °C for 24 h. Study shows that the hybrid exhibits high performance as both anode (firstly studied) and cathode materials for rechargeable lithium batteries. Electrochemical measurements revealed that the as-prepared Ag/Ag_{0.68}V₂O₅ hybrid displayed excellent cycling stability, especially as an anode material. The resulting anode retains 100% of the initial capacity after 1000 times under the current density of 400 mA g⁻¹. This phenomenon may be attributed to the electron conductivity improvement by the existence of metallic silver in the hybrid, and the convenient access to lithium ion ingress/egress by the unique structure.

1. Introduction

Lithium batteries (LBs), as one of the most important and promising energy storage portable devices, have gained more and more intensive interest in recent years.¹ Since the practical applications of LBs depend very closely on the long service life and reversible capacity of electrodes, how to improve the capacity and stability of electrodes become urgently needed for the development of LBs.²⁻³ Owing to their unique electrical properties, silver vanadium oxides (SVOs) have recently been extensively investigated in the field of LBs. For instance, Ag₂V₄O₁₁ is commercially used as the cathode material in lithium primary batteries for implantable cardioverter defibrillators (ICDs) because of its long-term stability and high specific capacity (315 mA h g⁻¹).⁴⁻⁶ β-AgVO₃ that has a higher Ag:V molar ratio is supposed to have better electrochemical properties as a cathode material.⁷ For examples, Chen et al. prepared Ag₂V₄O₁₁ nanowires, α-AgVO₃ microrods, and β-AgVO₃ nanowires through a simple and facile low-temperature hydrothermal approach.⁸ Electrochemical measurements reveal that β-AgVO₃ nanowires have much higher capacity (~100 mA h g⁻¹) above 3 V than that of Ag₂V₄O₁₁ nanowires and commercial Ag₂V₄O₁₁ bulk. Mai et al. used a one-step method based on β-AgVO₃ nanowires to synthesize silver vanadium oxides/polyaniline (SVO/PANI) triaxial nanowires, which exhibit enhanced electrochemical performance.⁹ They also designed a substrate-assisted hydrothermal approach in synthesizing mound-like radial β-AgVO₃ nanowire clusters on substrates.¹⁰ The capacity fading per cycle of this unique structure is only 0.17% at 500 mA g⁻¹, indicating that the prominent cycling stability of β-AgVO₃ at high discharge current. Although these SVOs have attracted extensive attention as cathodes for LBs,

little work has been focused on exploring other silver vanadium oxides as new potential electrodes (both anodes and cathodes) to meet the demand of higher capacity and better stability for rechargeable LBs in the SVOs family. It is well known that metal oxides (MOs) have been intensively studied as electrodes for lithium ion batteries because of their higher theoretical capacity than that of conventional graphite.¹¹ In particular, the 2D nanosheets structure of some MOs is reported beneficial for lithium storage,¹² which inspired us trying to synthesize SVOs with the 2D nanosheets structure and explore their potential application as an anode material for lithium storage.

Among the numerous SVOs, which contain Ag, V, and O in a number of stoichiometric and nonstoichiometric ratios, Ag_{0.68}V₂O₅ was first proposed as a potential electrode material in 1992.¹³⁻¹⁴ Its structure consists of layers that are composed of

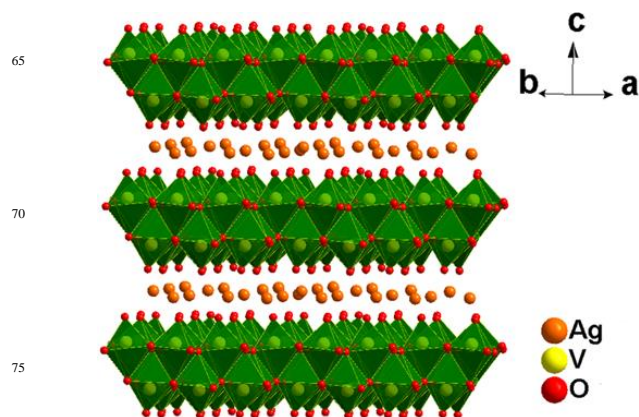


Figure 1. Schematic crystal structure of Ag_{0.68}V₂O₅ revealing the layered structure.

deformed VO₆ octahedra sharing edges and corners (Fig. 1).^{13,15} These layers have the composition V₂O₅ and are held together by means of silver ions. Each layer has two zig-zag ribbons of octahedra and is stacked along the z-direction. To our knowledge, this layer structured silver vanadium oxide, although investigated as a cathode material, has not been studied as an anode material for rechargeable LBs until now. This may be attributed to the poor cycling behavior commonly in SVOs.⁴⁻⁶ Recently, silver nanoparticles have been reported decorating on active materials to obtain good performance as electrodes. For instance, Takeuchi et al. revealed that silver ions in Ag₂VO₂PO₄ can be in-situ reduced to silver during discharge process, leading to high current capability of the material.¹⁶⁻¹⁸ Pan et al. prepared Ag/β-AgVO₃ hybrid nanorods before cycling, and found that this hybrid exhibited high discharge capacity, excellent rate performance and improved cycle stability.¹⁹ The enhanced performance can be ascribed to the good conductivity of the silver nanoparticles that result in better electron transportation.

In this work, we used a one-pot hydrothermal approach to synthesize peony-like Ag/Ag_{0.68}V₂O₅ hybrid with superior electrochemical properties as both anode and cathode materials for rechargeable LBs. An interesting formation process of the peony-like structure was discovered in only one hour. The effects of composition and structure of Ag/Ag_{0.68}V₂O₅ on the superior capacity and cycling stability were explored.

2. Experimental

2.1. Preparation of Ag/Ag_{0.68}V₂O₅ hybrid

All chemical reagents used in this work were analytical grade, commercially available from Shanghai Chemical Reagent Co., China, and used without further purification. In a typical procedure to synthesize the Ag/Ag_{0.68}V₂O₅ hybrid, yellow V₂O₅ (0.082 g), H₂C₂O₄ (0.170 g), and AgNO₃ (0.076 g) were added into a beaker containing distilled water (40 ml) under magnetically stirring at room temperature until the color of the solution became clear. Then, the resultant solution was transferred into a 60 ml autoclave with a Teflon liner and maintained at 180 °C for 24 h. After being naturally cooled down to ambient temperature, the final dark cyan precipitate was collected by centrifugation and washed with distilled water and ethanol for several times, respectively, then dried in a vacuum at 60 °C overnight. The time-dependent samples were synthesized similar to the Ag/Ag_{0.68}V₂O₅ hybrid except that reaction time was different. They were labelled as S1 (1 h), S2 (6 h), and S3 (12 h), respectively.

2.2. Physicochemical characterization of the samples

The X-ray powder diffraction (XRD) patterns were obtained on a Philips X'pert PRO SUPER diffractometer equipped with graphite monochromatized Cu Kα radiation (λ=1.541874 Å). The scanning electron microscopy (SEM) images were taken with a JEOL-JSM-6700F field emission scanning electron microscope. The transmission electron microscopy (TEM) images were recorded on a Hitachi Model H-7650 transmission electron microscope, using an electron kinetic energy of 100 kV. The energy dispersive X-ray spectra (EDS) were taken on a JEOL 2010 high-resolution transmission electron microscope performed

at an acceleration voltage of 200 kV. The chemical composition and the valence states of constituent elements were analyzed by an X-ray photoelectron spectroscopy (XPS; monochromatic Al Kα X-ray source, Kratos Analytical Ltd.).

2.3. Electrochemical characterization of the Ag/Ag_{0.68}V₂O₅ hybrid electrode

Electrochemical measurements were carried out using coin-type 2016 cells. For working electrodes, the Ag/Ag_{0.68}V₂O₅ hybrid was mixed with acetylene black, and polyvinylidene fluoride (PVDF) binder at a weight ratio of 70:20:10. The average loading of active material is approximately 1.5 mg. Lithium metal was used as the counter electrodes, and the separator was a Celgard 2400 microporous membrane. The electrolyte was 1 mol L⁻¹ LiPF₆ solution in ethylene carbonate and dimethyl carbonate solution (EC+DMC) (1:1) in volume. Cell assembly was carried out in a glove box filled with high-purity argon gas. Galvanostatic charge-discharge tests were performed on a LAND-CT2001A automatic battery tester (Wuhan, China) for a voltage window of 0.01-3.00 V and 1.50-3.50 V (vs. Li/Li⁺) at ambient temperature.

3. Results and Discussion

Figure 2 shows the XRD pattern of the product. As indexed in Figure 2, the (111), (200), (220) and (311) faces are well detected, which can be ascribed to the cubic phase Ag (JCPDS No. 04-0783).

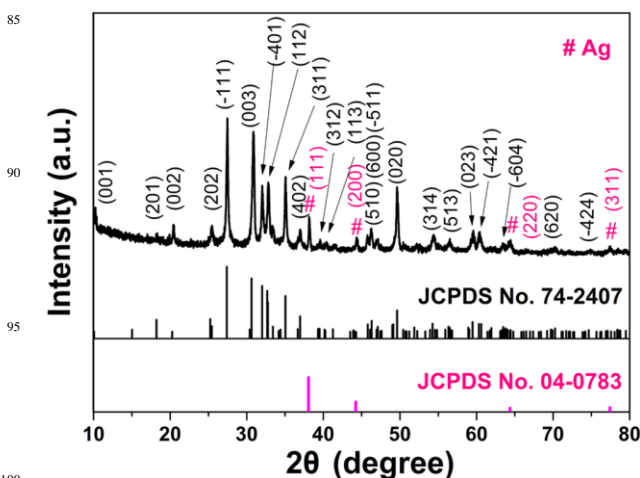


Figure 2. XRD patterns of the Ag/Ag_{0.68}V₂O₅ hybrid.

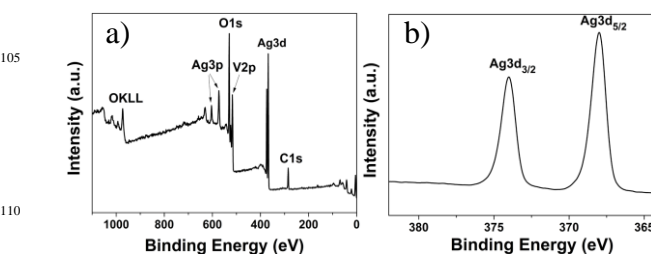


Figure 3. XPS spectra of Ag/Ag_{0.68}V₂O₅ hybrid: a) Survey

spectrum, b) Ag 3d.

0783). All the other diffraction peaks can be indexed to the monoclinic phase $\text{Ag}_{0.68}\text{V}_2\text{O}_5$ (JCPDS card 74-2407, space group C2/m). The XPS survey spectrum for the product is presented in Figure 3. The main peaks observed in the XPS survey spectrum (Figure 3a) were Ag 3d and 3p, V 2p and O 1s of the sample. Meanwhile, peaks for Ag 3d were also observed in Figure 3b. Both the peaks for Ag 3d_{5/2} and Ag 3d_{3/2} can be deconvoluted into two components, which indicates the presence of different valences of silver species.⁸ The element composition of the

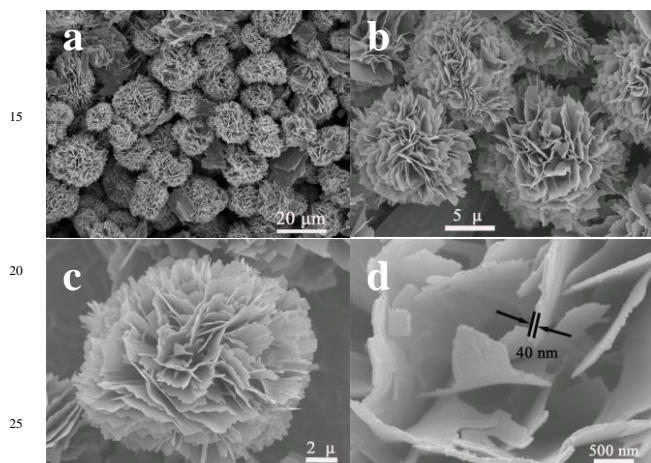


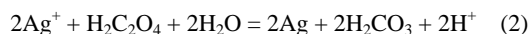
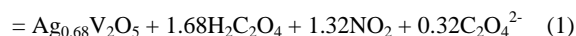
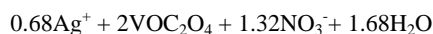
Figure 4. SEM images of the $\text{Ag}/\text{Ag}_{0.68}\text{V}_2\text{O}_5$ hybrid.

hybrid is studied by EDS and the result is shown in Figure S1. Ag and V elements are well detected. The atomic percentage of Ag and V elements are 29.36% and 70.64%, respectively. The Ag:V molar ratio is greater than the stoichiometric ratio of 0.68:2 of the $\text{Ag}_{0.68}\text{V}_2\text{O}_5$, suggesting the existence of silver.¹⁹

Figure 4 illustrates the representative SEM images of the $\text{Ag}/\text{Ag}_{0.68}\text{V}_2\text{O}_5$ sample. The panoramic image in Figure 4a indicates that the sample displayed a nanosheet stacking peony-

like morphology. Some independent nanosheets with irregular shape can be observed, which may be probably derived from the fragmentation of the $\text{Ag}/\text{Ag}_{0.68}\text{V}_2\text{O}_5$ hybrid during growth process. The high magnification SEM images shown in Figure 4b and 4c further reveals that these nanosheets were stacked regularly and densely to form peony-like morphology with a size of about 15 μm . The widths of these sheets were in a range of ~2 - 5 μm . The typical thickness of single sheet was approximately 40 nm that is marked by black arrows in Figure 4d.

We next carried out a time-dependent experiment to investigate the formation of peony-like $\text{Ag}/\text{Ag}_{0.68}\text{V}_2\text{O}_5$ hybrid in the present system. Only some diffraction peaks of $\text{Ag}_{0.68}\text{V}_2\text{O}_5$ were detected after a reaction time of 1 h (Figure 5a). When the reaction duration was prolonged to 6 h, several $\text{Ag}_{0.68}\text{V}_2\text{O}_5$ peaks became intensive along with the appearance of two diffraction peaks (111) and (200) of the Ag phase (Figure 5b). Further prolonging the reaction time to 12 h, the other two diffraction peaks (220) and (311) of Ag phase appears, which indicates the hybrid materials are mainly consisted of $\text{Ag}_{0.68}\text{V}_2\text{O}_5$ and Ag phase. Figure S4 shows the TEM images of the samples with different reaction time. As the reaction duration was prolonged, some nanoparticles were seen on the nanosheets of the hybrid, indicating the formation of the Ag particles. Based on the above analysis, the formation process of this $\text{Ag}/\text{Ag}_{0.68}\text{V}_2\text{O}_5$ hybrid can be described by the following two formulas:



According to the results of the studies above, formular (1) may be prior to formular (2) proceeding, as there were no diffraction peaks of silver phase in one hour. Figure 5d-f illustrates the formation process of the peony-like $\text{Ag}/\text{Ag}_{0.68}\text{V}_2\text{O}_5$ hybrid. As

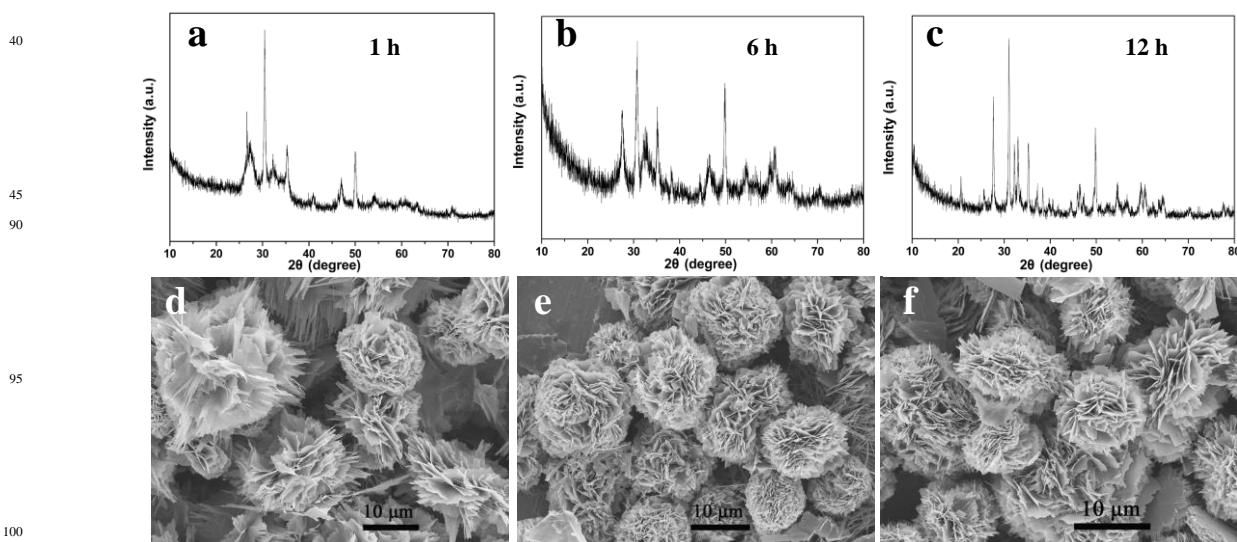
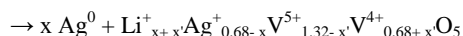
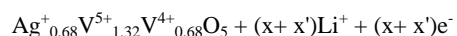


Figure 5. XRD patterns and SEM images of the time-dependent samples: a) and d) S1 (1 h), b) and e) S2 (6 h), c) and f) S3 (12 h).

shown in Figure 5d, the assembly of peony-like structures almost finished after the hydrothermal reaction of only one hour. As the reaction time prolongs, there appears no noticeable structural change of this peony-like structure (Figure 5e, 5f and 4a), indicating that this morphology can form quickly and hold its form well during aging processes.

Next, the peony-like Ag/Ag_{0.68}V₂O₅ hybrid is evaluated as a cathode material for LBs in view of its appealing structural features. Figure 6a shows the first three representative discharge-charge voltage profiles of the electrode at a current density of 35 mA g⁻¹ within a voltage window of 1.5-3.5 V. Two plateaus are observed at approximately 2.5 and 2.4 V in the first discharge curve. Lithium insertion seems to proceed mainly in two steps. The plateau located at 2.5 V can mainly be attributed to the reduction of Ag⁺ to Ag⁰ and the reduction of V⁵⁺ to V⁴⁺.²⁰ That means the existence of the simultaneous reduction from Ag⁺ to Ag⁰ and V⁵⁺ to V⁴⁺ in the first step. Ag⁺ between the V₂O₅ octahedrons layers are reduced to Ag⁰ that deposited as metallic silver, and the inserted lithium ions occupy the available sites between the layers.⁸ During the second plateau located at 2.4 V, the dominant reduction is from V⁴⁺ to V³⁺, as well partial reduction from V⁵⁺ to V⁴⁺.^{8,20} Based on these results, lithium insertion into the Ag/Ag_{0.68}V₂O₅ hybrid in each step is summarized by the following equations:

(i) in the first plateau ($0 \leq x \leq 0.68, 0 \leq x' \leq 1$)



(ii) in the second plateau ($0 \leq x'' \leq 0.32, 0 \leq x''' \leq 1.68$)

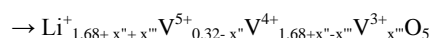
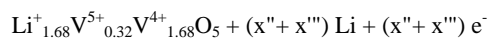


Figure S2a shows the cyclic voltammograms (CV) of this

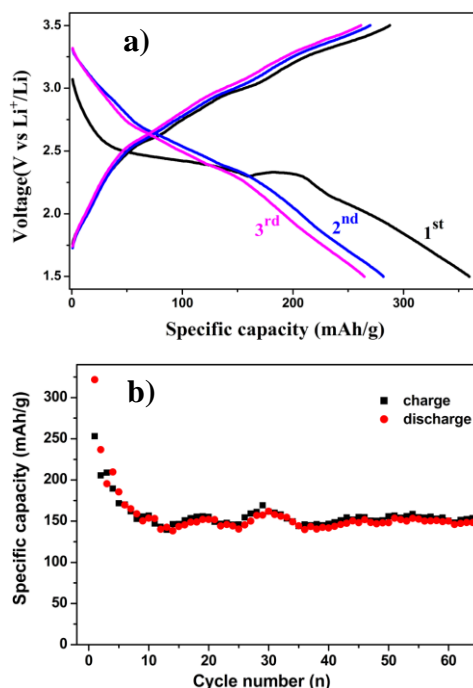


Figure 6. Electrochemical performances of the Ag/Ag_{0.68}V₂O₅ hybrid as a cathode material: a) Charge-discharge curves at a current density of 35 mA g⁻¹, b) Cycle performance at 0.1 A g⁻¹.

cathode made from the Ag/Ag_{0.68}V₂O₅ hybrid in the first three cycles at a scan rate of 1 mV s⁻¹ between 1.5 and 3.0 V. For the

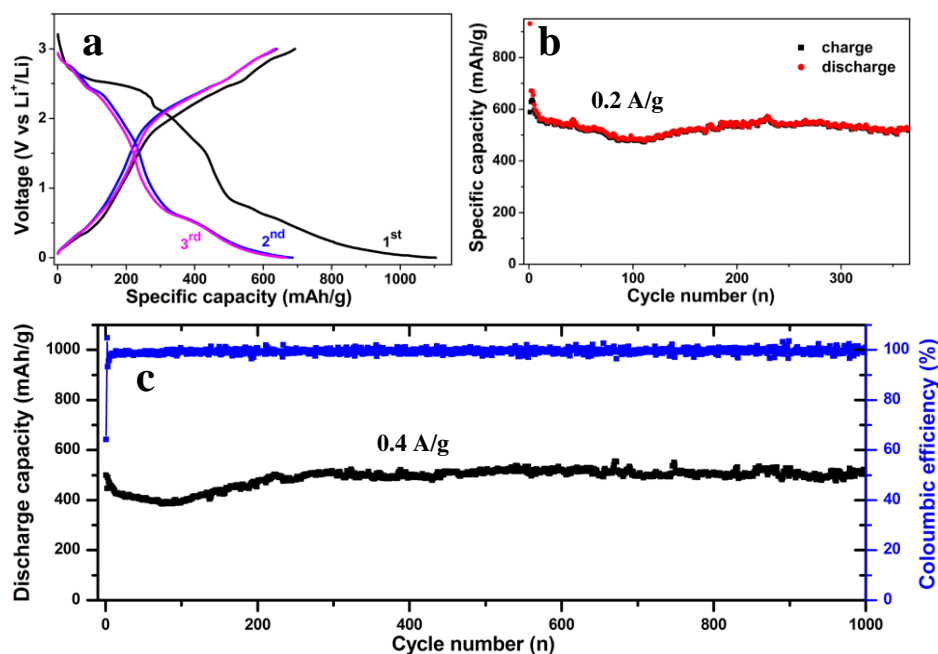


Figure 7. Electrochemical performances of the Ag/Ag_{0.68}V₂O₅ hybrid as an anode material: a) Charge-discharge curves at a current density of 0.1 A g⁻¹, b) Cycle performance at 0.2 A g⁻¹, and c) at 0.4 A g⁻¹.

first cycle, only one strong peak appeared at ~ 2.4 V when the electrode was scanned cathodically, and three main anodic peaks at 2.55, 2.95 and 3.20 V can be observed during the anodic sweep. From the second cycle, the CV curves mostly overlap, indicating the good reversibility of the electrochemical reactions, which is consistent with the discharge-charge voltage profiles (Figure 6a). The initial discharge and charge capacity is 360 and 288 mA h g⁻¹, respectively. The irreversible capacity loss can be attributed to the irreversible phase transformation after the initial cycle.¹⁹ During the first charging processes, there are two plateaus located at ~ 2.7 and 3.0 V, which may be resulted from the oxidation from V³⁺ to V⁴⁺ and V⁴⁺ to V⁵⁺.^{8,20} For the later cycles, the charge-discharge curves are generally overlapping, indicating the improved cycle stability. The cycling performance of the Ag/Ag_{0.68}V₂O₅ hybrid is presented in Figure 6b. The specific capacity stables at around 150 mA h g⁻¹ at the end of the 65th cycle after the first 15th fading. Compared with the good properties of V₂O₅ recently reported as a cathode material, 21-24 it should be noted that the lower voltage limit (1.5 V) and the significant capacity dropping during the first 10 cycles make this material less attractive as a cathode.

However, its potential possibility as an anode material for rechargeable LBs is firstly investigated in this work, which is shown in Figure 7. Before this assessment, we firstly tested the electrochemical impedance spectrum of the samples with different reaction time. As shown in Figure S5, the diameter of the semicircle for the sample (24 h) was much smaller than that of the other samples, indicating this product possessed lower charge-transfer resistance. The results further suggest that the introduction of Ag can enhance the electron conductivity of the materials. So, the sample with 24 h was chosen to evaluate its potential possibility as an anode material for rechargeable LBs.

Figure 7a shows typical charge-discharge curves for the first, second, and third cycles of the hybrid electrode at a current density of 100 mA g⁻¹ within a voltage window of 0.01-3.0 V. The plateaus of the initial discharge curve above 1.5 V are much similar to that in Figure 6a. When the discharge process proceeds deeply to the cut-off voltage of 0.01 V, the electrochemical activity may be the deep reduction of vanadium such as from V⁴⁺ to V³⁺, and V³⁺ to V²⁺ et al.. Such an overlapping phenomenon from the second cycle was also observed in the cyclic voltammograms of this anode located between 0.01 and 3.00 V (Figure S2b). The first discharge capacity is 1104 mA h g⁻¹, while the corresponding first charge capacity is 693 mA h g⁻¹, which gives an initial Coulombic efficiency (CE) of 62.8%. The irreversible capacity loss of 37.2% may be mainly ascribed to irreversible processes such as phase transformation and inevitable formation of solid electrolyte interface (SEI) film. Like those high-capacity metal oxide based anode materials, the Ag/Ag_{0.68}V₂O₅ electrode also has the common drawback of the relatively poor initial CE, which requires some efforts to improve in practical applications. The charge-discharge curves are quite similar from the second cycle, which indicates the enhanced cycle stability and the rapidly increased CE of 93.3%. Figure 7b shows the cycling performance at a current density of 200 mA g⁻¹ between 0.01 and 3.0 V. The discharge capacity gradually decreases and stabilize at about 480 mA h g⁻¹ after 110 cycles.

Then, the capacity starts to increase and reaches a value of 570 mA h g⁻¹ in the 230th cycle, and could stabilize at around 530 mA h g⁻¹ after 365 cycles. Such an interesting phenomenon is also observed in Figure 7c.

As shown in Figure 7c, the cycling performance together with the CE of the Ag/Ag_{0.68}V₂O₅ sample is evaluated at a current density of 400 mA g⁻¹. Though the initial CE is around 65%, it will quickly increase and remain as nearly 100% thereafter. The reversible capacity stabilizes and retains at 385 mA h g⁻¹ in the 75th cycle, and can recover back up to 520 mA h g⁻¹ after 1000 cycles. This dropping-rising phenomenon that happened along with the cycling process could be attributed to the presence of a possible electrochemical activation process in the electrode material.²⁵⁻²⁷ From the 200th cycle onwards, the as-prepared Ag/Ag_{0.68}V₂O₅ hybrid exhibits excellent cyclic capacity retention with a stable reversible capacity around 500 mA h g⁻¹, which corresponds to a remarkable retention of 100% of the initial discharge capacity after 1000 cycling times. A comparison of the electrochemical performance of our peony-like Ag/Ag_{0.68}V₂O₅ hybrid with some representative reported SVOs electrode materials is given in Table S1. The superior electrochemical performance of this peony-like sample demonstrates the beneficial effects of such a unique hierarchical structure.^{10,28} Firstly, the nanosheet building blocks with small thickness greatly facilitate intercalation and deintercalation of lithium ions because of the short diffusion length;¹⁰ secondly, the hierarchical structure composed of nanosheets not only reduce the self-aggregation of the electrode materials,²⁸ but also increases the contact area between the active material and electrolyte, thus leading to the better electrochemical performance.²⁸ Moreover, the metallic silver that existed in the hybrid can increase the electronic conductivity of the Ag_{0.68}V₂O₅, which is also beneficial for the good cycling performance of the electrode materials at a relatively high rate (400 mA g⁻¹).¹⁹

To demonstrate the structural stability that ensures the superior electrochemical properties upon prolonged cycling, we analyzed the SEM images of the Ag/Ag_{0.68}V₂O₅ electrode after 1000 cycles. As shown in Figure 8, the sample still keeps the nanosheet morphology without obvious self-aggregation. The similar results were also found on the morphologies of this hybrid as a cathode material after a few cycles, as shown in Figure S3. It is

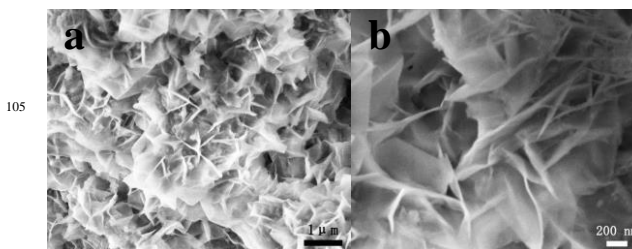


Figure 8 SEM images of the Ag/Ag_{0.68}V₂O₅ hybrid after 1000 cycles as an anode material.

believed that the high surface energy of nanoscaled electrode materials is a reason for self-aggregation, which could reduce the

effective contact areas of active materials and electrolytes, and result in capacity fading sharply. However, our peony-like Ag/Ag_{0.68}V₂O₅ hybrid with the hierarchical structure effectively reduced the self-aggregation and greatly sustained the cycling stability of the electrode materials.

4. Conclusions

In summary, a facile one-pot solvothermal method has been developed to synthesize the peony-like Ag/Ag_{0.68}V₂O₅ hybrid. When evaluated as both anode and cathode materials for rechargeable LBs, the hybrid exhibit remarkable cycling stability. The enhanced electrochemical performance can be attributed to the electron conductivity improvement by the existence of silver in the hybrid, and the hierarchical structure with nanosheet subunits and hollow interior.

15 Acknowledgements

This work was supported by the 973 Project of China (No. 2011CB935901), the National Natural Science Fund of China (No. 91022033, 21201158), Anhui Provincial Natural Science Foundation (1208085QE101).

20 Notes and references

^a Hefei National Laboratory for Physical Science at Microscale and Department of Chemistry, University of Science and Technology of China, Hefei, 230026, P.R. China. Tel: +86-551-63601589; E-mail: ychzhu@ustc.edu.cn

^b School of Chemistry and Chemical Engineering, Shandong University, Jinan, 250100, PR China. Tel: +86-551-63607234; E-mail: ytqian@ustc.edu.cn

[†] These authors contributed equally to this work.

[†] Electronic Supplementary Information (ESI) available. See DOI: 10.1039/b000000x/

[‡] Footnotes should appear here. These might include comments relevant to but not central to the matter under discussion, limited experimental and spectral data, and crystallographic data.

1 Dunn, B.; Kamath, H.; Tarascon, J.-M., *Science* **2011**, *334*, 928.

2 Reddy, M.; Subba Rao, G.; Chowdari, B., *Chem. Rev.* **2013**, *113*, 5364.

3 Tarascon, J.-M.; Armand, M., *Nature* **2001**, *414*, 359.

4 Skarstad, P. M., *J. Power Sources* **2004**, *136*, 263.

40 5 Crespi, A.; Schmidt, C.; Norton, J.; Chen, K. M.; Skarstad, P., *J. Electrochem. Soc.* **2001**, *148*, A30.

6 Leising, R. A.; Takeuchi, E. S., *Chem. Mater.* **2394**, *6*, 489.

7 Takeuchi, E. S.; Piliero, P., *J. power Sources* **2387**, *21*, 133.

8 Zhang, S.; Li, W.; Li, C.; Chen J., *J. Phys. Chem. B* **2006**, *110*, 24855.

45 9 Mai, L.; Xu, X.; Han, C.; Luo, Y.; Xu, L.; Wu, Y. A.; Zhao, Y., *Nano Lett.* **2011**, *11*, 4992.

10 Han, C.; Pi, Y.; An, Q.; Mai, L.; Xie, J.; Xu, X.; Xu, L.; Zhao, Y.; Niu, C.; Khan, A. M.; He, X., *Nano Lett.* **2012**, *12*, 4668.

50 11 Wu, H. B.; Chen, J. S.; Hng, H. H.; Lou, X. W., *Nanoscale* **2012**, *4*, 2526.

12 Chen, J. S.; Lou, X. W., *Materials Today* **2012**, *15*, 246.

13 Garcia-Alvarado, F.; Tarascon, J.-M.; Wilkens, J., *J. Electrochem. Soc.* **2392**, *139*, 3206.

55 14 Garcia-Alvarado, F.; Tarascon, J.-M., *Solid State Ionics* **1993**, *63/65*, 401.

15 Andersson, S., *Acta Chem. Scand.* **1965**, *19*, 1371.

16 Marschilok, A. C.; Takeuchi, K. J.; Takeuchi, E. S., *Electrochem. Solid-State Lett.* **2009**, *12*, A5.

60 17 Marschilok, E. S.; Marschilok, A. C.; Tanzil, K.; Kozarsky, E. S.; Zhu, S.; Takeuchi, K. J., *Chem. Mater.* **2009**, *21*, 4934.

18 Marschilok, A. C.; Kozarsky, E. S.; Tanzil, K.; Zhu, S.; Takeuchi, K. J.; Takeuchi, E. S., *J. Power Sources* **2010**, *195*, 6839.

65 19 Liang, S.; Zhou, J.; Pan, A.; Zhang, X.; Tang, Y.; Tan, X.; Chen, T.; Wu, R., *J. Power Sources* **2013**, *228*, 178.

20 Kawakita, J.; Sasaki, H.; Eguchi, M.; Miura, T.; Kishi, T., *J. Power Sources* **1998**, *70*, 28.

21 Pan, A. Q.; Wu, H. B.; Yu, L.; Lou, X. W., *Angew. Chem., Int. Ed.* **2013**, *52*, 2226.

70 22 Wu, H. B.; Pan, A. Q.; Hng, H. H.; Lou, X. W., *Adv. Funct. Mater.* **2013**, *23*, 5669.

23 Zhang, C. F.; Chen, Z. X.; Guo, Z. P.; Lou, X. W., *Energy Environ. Sci.* **2013**, *6*, 974.

75 24 Pan, A. Q.; Zhu, T.; Wu, H. B.; Lou, X. W., *Chemistry-A European Journal* **2013**, *19*, 494.

25 Laruelle, S.; Grugeon, S.; Pizot, P.; Dolle, M.; Dupont, L.; Tarascon, J.-M., *J. Electrochem. Soc.* **2002**, *149*, A627.

80 26 Grugeon, S.; Laruelle, S.; Dupont, L.; Tarascon, J.-M., *Solid State Sci.* **2003**, *5*, 895.

27 Zhang, G.; Yu, L.; Wu, H. B.; Hoster, H. E.; Lou, X. W., *Adv. Mater.* **2012**, *24*, 4609.

28 Pan, A. Q.; Wu, H. B.; Zhang, L.; Lou, X. W., *Energy Environ. Sci.* **2013**, *6*, 1476.